Behavior of Ir atoms and clusters on Ir surfaces

Chong-lin Chen and Tien T. Tsong
Department of Physics, The Pennsylvania State University, University Park, Pennsylvania 16802
(Received 19 July 1989; revised manuscript received 24 January 1990)

Several aspects of the behavior of single Ir atoms and small Ir atomic clusters on the Ir(100) and Ir(111) surfaces as functions of the temperature have been studied with the atomic-resolution field-ion microscope. From these experiments, diffusion parameters, the dissociation energy of plane edge atoms, and other experimental parameters of interest have been derived. For very small clusters, the probabilities of observing different structures, in general, depend on the temperature. For the three-atom cluster on the Ir(111) the $\ln(p_{1D}/p_{2D})$-vs-$(1/T)$ plot, where p_{1D} and p_{2D} represent, respectively, the probabilities of forming a one- and a two-dimensional structure, is linear. The 2D structure is more stable with a larger effective cluster binding energy of 0.098 ± 0.004 eV. In contrast, for the three-atom Ir cluster on the Ir(100) the plot exhibits two linear sections, one with an effective cluster binding-energy difference of $\sim0.335\pm0.015$ eV, and one is equivalent to have an effective cluster binding-energy difference of $\sim3.94\pm0.35$ eV. The 1D structure is more stable. We believe that this deviation from the simple linear behavior on the (100) surface is due to the occurrence of a structure phase transition of the three-atom cluster interacting with the substrate, which is a large reservoir containing many atoms. The dissociation energy of plane edge atoms, or the 2D sublimation energy, of the Ir(100) layer is found to be ~1.4 eV, from which the binding energy of Ir adatoms on the Ir(100) surface is derived to be ~6.5 eV.

I. INTRODUCTION

Fundamental to the understanding of many surface phenomena and nucleation and growth of crystals is how single atoms and small atomic clusters behave on solid surfaces, and what are the energies involved in different atomic processes.[1,2] These atomic processes include surface diffusion of single atoms, interaction of single atoms with the substrate and with one another, stepping up and down a lattice step of single atoms, association of single atoms into clusters and dissociation of clusters into single atoms and small atomic clusters, and aggregation of clusters into a surface layer, and dissociation of a surface layer or the two-dimensional thermal desorption of atoms from plane edges, etc. Field-ion microscopy (FIM),[3] with its ability to image individual atoms on a surface with atomic resolution and to produce a well-characterized surface by low-temperature field evaporation, and its relative ease in changing the surface temperature, is ideally suited for studying surface atomic processes quantitatively, and in fact many such studies have already been reported.[4] Here we report a study of a variety of atomic processes of single Ir atoms and small Ir clusters on the (1×1), or the nonreconstructed, Ir(100) and Ir(111) surfaces.

In the past, most FIM studies of the behavior of single atoms and small atomic clusters were performed on the bcc tungsten (110) surface. A few studies reported for fcc surfaces were mainly restricted to the measurement of surface diffusion parameters.[5,6] Only very recently, a few studies of the formation of clusters on fcc surfaces have been reported.[7] From the theoretical point of view, fcc lattices are much more easily treated than bcc lattices, and most molecular-dynamics simulations of surface atomic processes are performed on fcc surfaces.[8] The purpose of the present study is to extend the FIM study of atomic processes to fcc surfaces, and also to carry out some new studies which either have not yet been done, or have not yet been done in any detail.

II. EXPERIMENTAL METHODS

Experimental methods and procedures for FIM experiments with single atoms on metal surfaces have been well established from years of such studies. Details can be found in the literature[4] and will not be further described here. In the present study, we again pay great attention to the vacuum condition, and the thorough degassing of the deposition sources. Vacuum below 5×10^{-11} Torr is always maintained from repeated bake-out of the system.

Two methods of tip heating are used in this experiment. One uses a Lexel Model-85 Cu-ion cw Laser and the other uses an electronically controlled pulsed-voltage power supply for joule heating of the tip mounting loop. The laser unit has the maximum power of 0.5 W with the spectrum centered around $\lambda=5145$ Å. The output power can be continuously adjusted. With our laser focusing setup, a power in the range of 0–500 mW is needed to heat the tip all the way from ~20 to over 600 K. The advantage of laser heating is that a final heating temperature can be reached in the μs range if the heated spot is very small.[9] The quenching time is also much faster in the microsecond to the millisecond range. Thus the length of the heating period can be adjusted all the way from ~0.1 s or less to over 1 min by simply chopping the laser beam with a mechanical chopper. The final temper-

 ©1990 The American Physical Society

ature reached can be calibrated according to the temperature dependence of the evaporation field of the tip surface.[10] Another advantage is that only a very small spot of the tip is heated. Thus contamination of the field-evaporated part of the emitter surface by degassing from other parts of the FIM is minimized. The disadvantage of the laser-heating method is that there are some problems with the long-term stability of the laser. Also, an accurate absolute temperature calibration is difficult, even though the precision of measuring temperature changes is as good as that given by the electric current heating methods. The precision in both methods is better than ± 0.2 K. Thus the laser-heating method is not suited for studying quantitatively atomic processes which can occur at very low temperatures. In such cases, a small inaccuracy in the temperature calibration can induce a large error in the measurements.

In Fig. 1 we show how the final heating temperature of the tip varies with the laser power, and in Fig. 2 we show an Arrhenius plot for surface diffusion of single tungsten atoms on the tungsten (110) surface derived with the laser-heating method. The diffusion parameters derived from this plot are $E_d = 0.91 \pm 0.03$ eV and $D_0 = 1.2 \times 10^{-2} \times (9^{\pm 1})$ cm^2/s. These values are in fair agreement with those obtained by the resistivity heating methods.[4] All the other data presented in this paper, however, are obtained with an electronically controlled pulsed-voltage dc power supply. With this power supply, the final heating temperature can be reached in less than 0.1–0.2 s without an overshoot. This is very important, since the logarithmic rate of atomic processes usually depends on the inverse temperature of the surface. In our experimental measurements, the heating period is set at 20 s. The quenching rate at the tip apex is estimated to be ~ 100 K/s near the heating temperature. During heating, no image field is applied. At the imaging temperature, 20–30 K, repeated applications of the image field will not change either the position of an adatom or cluster nor the structure of a cluster. We used diffused He of pressure $\sim 5 \times 10^{-5}$ Torr for the field-ion imaging. No structure changes of clusters by field adsorption of either helium or neon have ever been observed at a surface temperature of 20 to 30 K in all metal cluster studies.

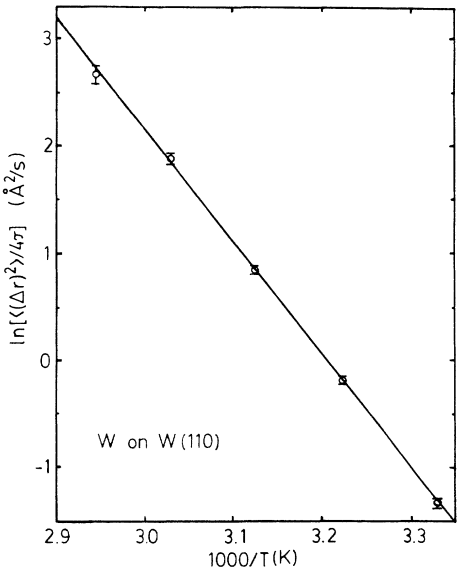

FIG. 2. Arrhenius plot for the diffusion of a W atom on a W(110) surface obtained with the laser-heating method.

In the course of this investigation, we also find an interesting image spot shape of single Ir adatoms on the Ir(111) surface. While in the past, single atoms of different species deposited on various surfaces all show circular image spot shape, single Ir adatoms on the Ir(111) show a triangular image spot shape as can be seen in Fig. 3. Whereas this will not affect in any way our study of atomic processes, it is an interesting phenomenon worthy of further study. Two different mechanisms may be responsible for the triangular image spot shape. It may be caused by the resonating motion of a field adsorbed image gas atom along the three ⟨110⟩ atomic row directions of the substrate. It may also be caused by a triangular spatial distribution of the electronic charge density of the substrate around an adatom right

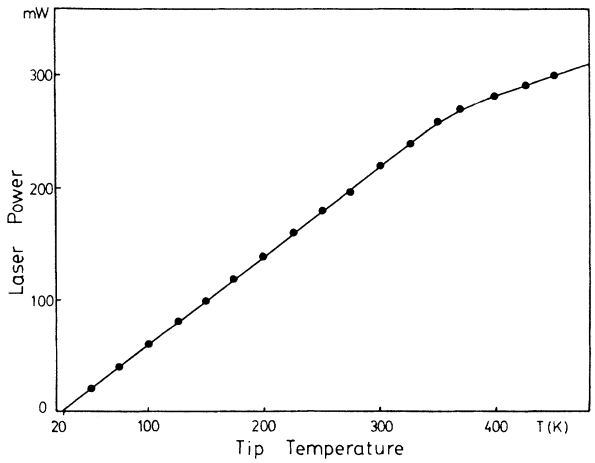

FIG. 1. Final tip temperature vs laser power in laser heating for a tungsten tip.

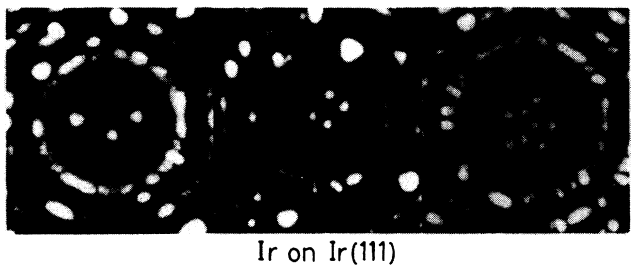

FIG. 3. A few helium-ion micrographs showing the triangular image spots for Ir adatoms on the Ir(111) surface.

above the Fermi level, known as Friedel oscillation of electronic charges around an adsorbed atom. The fcc (111) surface, of course, has a three fold symmetry in the atomic arrangement. As the former effect may be closely related to the latter, such a distinction may be somewhat artificial. A similar observation has been reported earlier by Page and Ralph for retained Rh atoms on the (100) surface of Ir-Rh alloys which shows an image intensity tail in the four [110] directions of the surface. They attribute this cusp shaped image spot to Friedel oscillation of electronic charges around an impurity Rh atom.[11]

III. RESULTS AND DISCUSSIONS

A. Surface diffusion

The most thoroughly studied of all surface atomic processes is surface diffusion.[4] Our study of surface diffusion is for the purpose of complementing the study of other atomic processes. The surface-diffusion parameters of single Ir adatoms on the Ir(100) and Ir(111) planes are derived by depositing one adatom on a plane, and by using pulsed-current heating of the tip mounting loop to induce surface diffusion in the absence of an image field. Figure 4 shows some FIM images of an Ir adatom on a (100) surface in the diffusion process. Each data point consists of over 100 heating periods of measurements. The Arrhenius plots obtained are shown in Fig. 5. The activation energies and diffusivities derived from the slopes and the intercepts of these plots for the (100) and (111) planes are, respectively, $E_d=0.93\pm0.04$ eV and $D_0=1.4\times(10^{\pm1})\times10^{-2}$ cm^2/s, and $E_d=0.022\pm0.03$ eV and $D_0=8.84\times(8^{\pm1})\times10^{-3}$ cm^2/s. Thus, within the accuracy of the FIM measurements, D_0 is on the order of kTl^2/h, where l is the jump length of ~2.8 Å, as has been concluded earlier from compiling the FIM data then available.[12] At the present time, the accuracy of FIM determination of D_0 is very limited because of the small temperature range in which a measurement can be conveniently done. It is quite clear that the activation energy of surface diffusion for Ir adatoms is very much lower on the smooth (111) plane than on the relatively rough (100) plane, similar to the self-diffusion of Rh on Rh surfaces.[5]

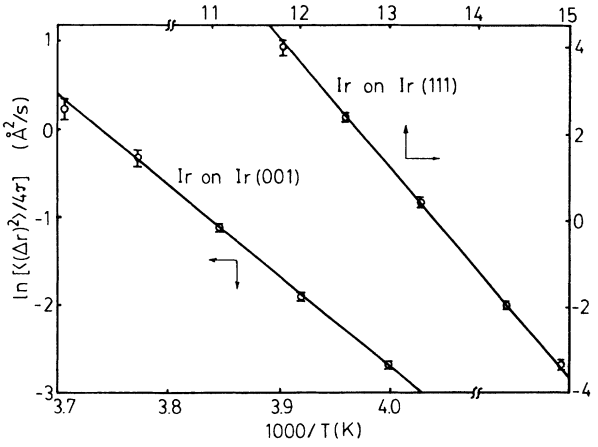

FIG. 5. Arrhenius plots for surface diffusion of an Ir adatom on an Ir(100) and an Ir(111) surface.

Diffusion parameters can, of course, be derived for small clusters if one uses the center of mass of clusters for determining the mean-square displacements. Since this would be another time-consuming study and surface diffusion is not the main concern of this study, we have not yet carried out these measurements. During the course of our study of cluster structures and structure transformations on the Ir(111) plane, we did notice that

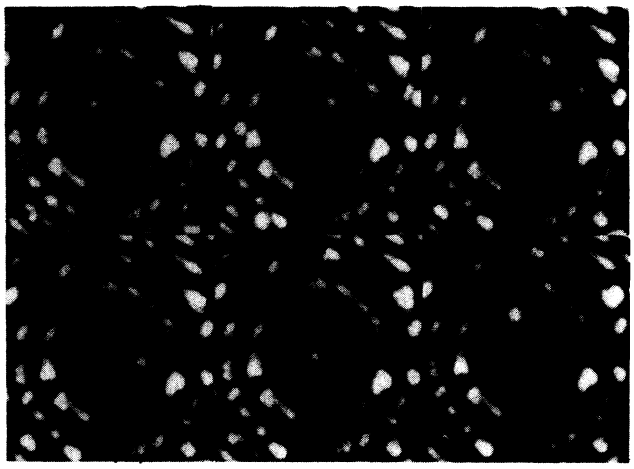

FIG. 4. FIM images showing 2D random walk surface diffusion of an Ir adatom on an Ir(100) surface.

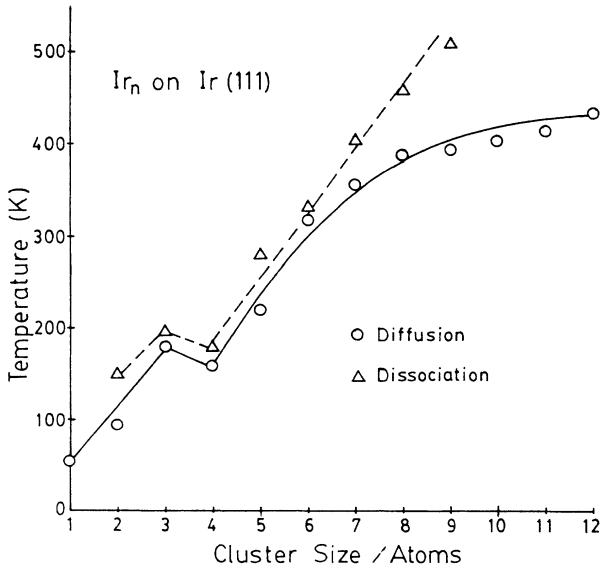

FIG. 6. The "onset" diffusion temperature and the dissociation temperature of Ir clusters of different sizes.

the "onset" temperature, defined approximately as the temperature where $\langle(\Delta r)^2\rangle^{1/2}/t \simeq 0.5$ Å/s, increases montonically from about 60 to 435 K when the size of the clusters increases from 1 to 12 atoms, as shown in Fig. 6. However, for three- and four-atom clusters, this temperature is reversed. As will be discussed later, the dissociation temperature of clusters on this surface also shows a similar reversed feature for the three-atom and four-atom clusters.

B. Formation and behavior of small atomic clusters

When diffusing atoms encounter each other, very often they will combine into a cluster.[4] At a given temperature, clusters can assume certain structures, and transformation from one structure to another can occur. In an early experiment it was concluded that the structures of clusters depend very sensitively on the surface temperature.[13] For example, it was observed that a six-atom cluster of W on the W(110) surface assumed a highly symmetric structure below 390 K. Above this temperature, a less symmetric structure was formed. Changes in the orientation or the position of the cluster could occur, but it never returned to the low-temperature structure. Bassett[14] found that on the W(110), Ni, Pd, Ir, and Pt adatoms initially nucleated as linear chains oriented in the direction of the closely packed atomic rows of the W(110) surface. Beyond a critical number of near ten atoms, the linear chains would transform into 2D clusters or small islands. Schwoebel and Kellogg[7] reported a study of the stability of Ir clusters on the Ir(001) surface. They found that if the number is less than or equal to five, the stable structures are one dimensional. For clusters of greater than or equal to six atoms, the stable structures become two dimensional. From a statistical mechanics point of view, as the number of atoms in a cluster is very small, one may not expect a well-defined temperature nor a well-defined critical-atom number, as can be expected from critical phenomena of large systems, in the structure transformation of small clusters. One would expect that, in general, the probabilities of observing different structures of clusters to depend on the surface temperature. If a structure phase transition occurs, its behavior should exhibit a strong size effect, which can be studied with the field-ion microscope. Few of the earlier studies of cluster structure transformation are, however, quantitatively significant. These are some of the motivations for this study.

1. Cluster structures and structure transformation on Ir(100)

In Fig. 7, the atomic structure of the Ir(100) is shown. Typically unless the tip radius is very small and the top surface layer is also very small, the atomic structure of the surface is not resolved in the FIM. However, when small clusters are formed, as long as the tip radius is not too large, all the atoms in the clusters can be resolved, as shown in Fig. 8, for three- and four-atom clusters. In general we find the Ir clusters formed at low temperatures on the Ir(100) to be linear, lining up in the ⟨110⟩ directions, as previously reported.[7] Transformation to

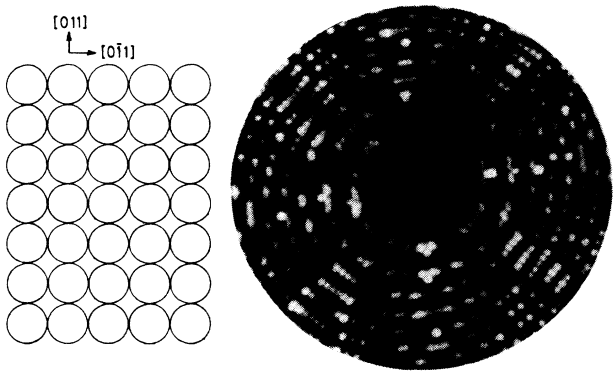

FIG. 7. The atomic and image structures of the Ir(100) surface. Each ring represents a surface layer.

2D structure can occur if the temperature is high enough. For small clusters of a given size, the probability of observing a 1D or a 2D structure depends on the temperature of the surface in a continuous manner. We do not observe a well-defined critical number, found to be six in an earlier study,[7] nor a very-well-defined temperature in the 1D to 2D transformation of small Ir clusters on the Ir(100) surface. Figure 9 shows a linear six-atom cluster formed from combining three two-atom clusters at ~380 K. Upon heating to 420 K, it transforms into a 2D structure. Heating to 470 K for one period, the cluster changes its orientation. With two additional periods of heating to 470 K, it transforms back into the 1D linear chain structure. In fact, for the nine-atom cluster, the high-temperature structure is one dimensional, as shown

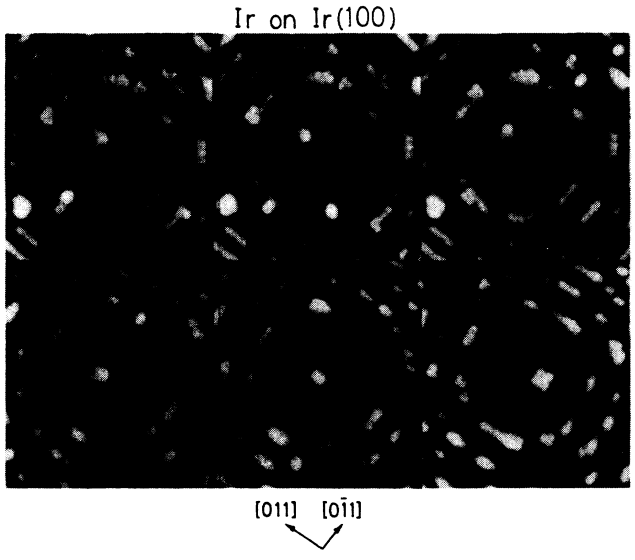

FIG. 8. Images of three- and four-atom Ir clusters on the Ir(100) surface. In a field-ion image, the magnification of a small atomic cluster is usually much larger than the overall magnification of the image.

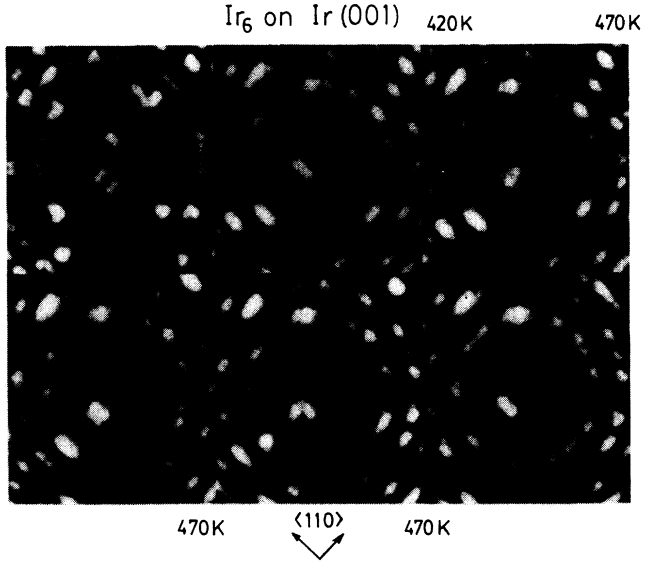

FIG. 9. Images of a six-atom Ir cluster on the Ir(100) surface and its structure changes at different heating temperatures.

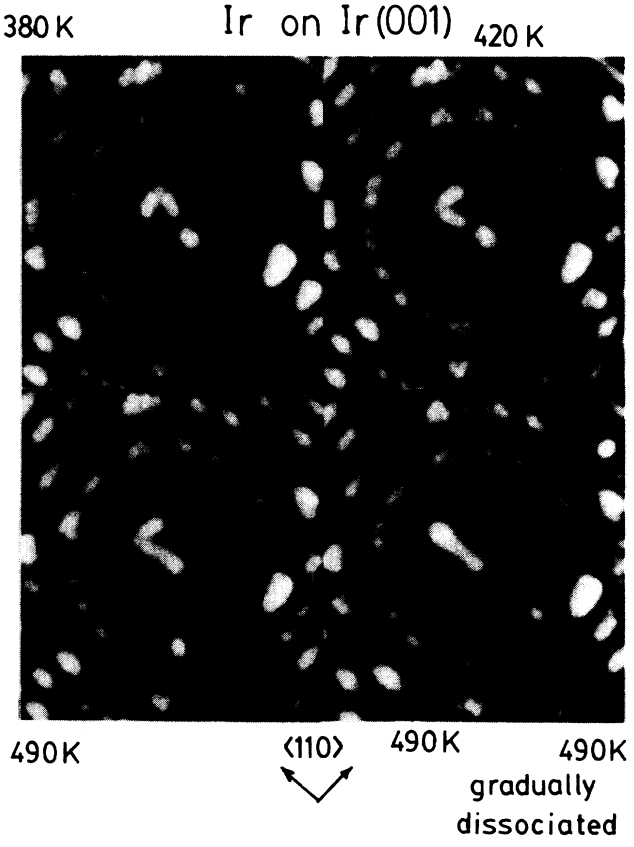

FIG. 10. Image of a nine-atom Ir cluster on the Ir(100) surface showing various stages of structure changes.

TABLE I. Three-atom Ir clusters on Ir(001).

T (K)	No. of 1D clusters	No. of 2D clusters	p_{1D}/p_{2D}
377.5	635	7	90.7±0.4
380.0	359	15	23.9±0.3
382.5	178	15	11.9±0.2
385.0	168	22	7.6±0.2
387.5	117	18	6.5±0.2
392.5	182	32	5.7±0.1
405.0	248	54	4.6±0.1
417.5	124	35	3.5±0.1

in Fig. 10. No true 2D structure is observed for this cluster.

As explained earlier, since the number of atoms in a cluster is very small, singularity behaviors such as those found in critical phenomena of large systems may not be expected. Instead, one may expect the probabilities of observing a 1D and a 2D cluster structure to be temperature dependent. For six-atom clusters, we found that at 375 K, $p_{1D}/p_{2D}=20/1$. At 490 K, it is $\frac{21}{9}$ and at 505 K, it is $\frac{17}{6}$. Large clusters are difficult to study quantitatively because of the different 2D structures formed, and also because of the gradual loss of atoms by dissociation during an experimental measurement at high temperatures. We have made a quantitative study of the three-atom cluster which is the smallest cluster still exhibiting a 1D to 2D cluster structure transformation. For the three-atom cluster, two quantitatively reliable sets of data, out of a total of ~4000 heating periods of observations, have been obtained from two Ir tips and thus with two independent temperature calibrations. One set is listed in Table I, and the other set is shown in Fig. 11. Assuming that no redistribution occurs during the quenching of the

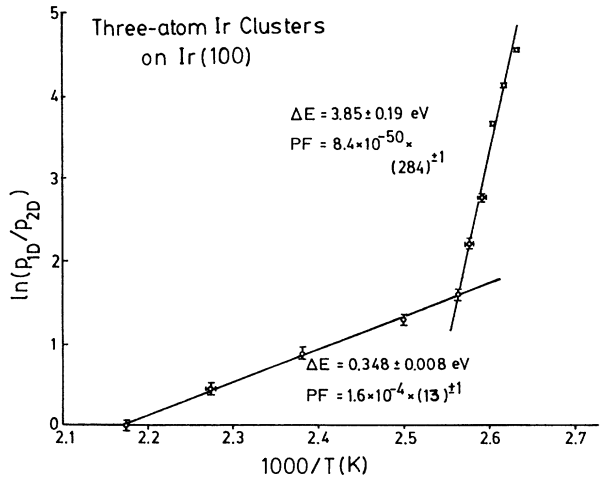

FIG. 11. Temperature dependence of the probabilities of observing a 1D and 2D structure of the three-atom Ir cluster on the Ir(100) surface.

tip, the ratio of these probabilities will then follow the Boltzmann statistics according to

$$p_{1D}/p_{2D}=(W_1/W_2)\exp(\Delta E_{12}/kT)\ , \quad (1)$$

where W_1 and W_2 represent, respectively, the statistical weights of the 1D and 2D structures, and $\Delta E_{12}=E_1-E_2$ is the difference in the total cluster binding energies (magnitudes), or internal energies, of the cluster in the 1D and 2D structures. One therefore can expect a simple linear $\ln(p_{1D}/p_{2D})$ versus $1/T$ plot. To our great surprise, however, this plot exhibits two distinctive linear sections, as seen in Fig. 11. The fractional statistical uncertainty of each data point is calculated from a standard equation for the ratio of two random events, as that used for calculating the uncertainty in a measurement of the composition of a two-component system by a particle-counting method. This fractional uncertainty is given by $\sigma=(n_1n_2)^{1/2}/(n_1+n_2)^{3/2}$, where n_1 and n_2 are, respectively, the numbers of the 1D and 2D structures. One section has a slope of $(4040\pm94\text{K})k$, which corresponds to a ΔE_{12} of 0.348 ± 0.008 eV, and a preexponential factor of $1.6\times(13)^{\pm1}\times10^{-4}$ and a linearity of 0.9973. The other section has a slope of $(44733\pm2176\text{K})k$, which corresponds to a ΔE_{12} of 3.85 ± 0.188 eV and a preexponential factor of $8.4\times(284)^{\pm1}\times10^{-50}$ and a linearity of 0.9860. The transition occurs at $\sim$388 K. The set of data listed in Table I gives a similar result of 0.322 ± 0.021 eV and $4.4\times(13)^{\pm1}\times10^{-4}$ and 0.9402 for one section, and 4.02 ± 0.51 eV and $1.5\times(361)^{\pm1}\times10^{-52}$ and 0.9796 for the other section.

On metal surfaces, adatom-adatom interactions have pair energies always on the order of 0.1 eV.[4] Thus a difference in the total cluster binding energies of the order of ~0.335 eV for the 1D and 2D three-atom clusters, derived from the high-temperature section, is quite reasonable. A ratio of the statistical weights of $\sim10^{-4}$ is not unreasonable either if one considers the possible difference in the phase space of the two states. That the 1D cluster has a larger total binding energy is also consistent with the earlier conclusion that below six atoms, 1D structures are the stable ones. A puzzling question is why the low-temperature section exhibits such a large difference in the cluster binding energies of ~3.94 eV. We believe that this section merely signifies a significant deviation from the simple linear behavior of the plot, and the slope of this section may not truly represent an energy difference. In other words, Eq. (1) is oversimplified and it does not validly describe the structure changes of a small atomic cluster which interacts strongly with the substrate containing a very large number of atoms. Even though the structure of the substrate remains unchanged, the elastic distortion of the lattice induced by the 1D three-atom cluster must be quite different from that induced by the 2D three-atom cluster. Thus neither the slope nor the prefactor of the low-temperature section has a simple physical meaning of a simple Arrhenius plot as given by Eq. (1), which is valid only for describing the structure distribution of a thermally equilibrated ensemble of three-atom clusters, not three-atom clusters interacting with the substrate. It would be interesting for theorists to look into this problem more carefully and provide us with valid equations. Our analysis is based on the assumption that no redistribution occurs during the quenching process; therefore the energies calculated with use of Eq. (1) are effective energies.

Obviously the large deviation from a simple linear Arrhenius behavior observed will affect the detailed atomic steps in the nucleation and growth of surface layers and many other surface atomic processes on this surface. The observation of this novel behavior also demonstrates that size effects in structure transition of small atomic clusters, or systems containing only a few particles, interacting with the substrate by inducing lattice distortion around the cluster, or coupled to a reservoir of very large size, can be studied with the FIM. These effects are fundamentally interesting problems for experimental and theoretical studies.

2. *Cluster structures and structure transformation on the Ir(111)*

The Ir(111) plane has a closely packed stucture, as shown in Fig. 12. Again, the atomic structure of the substrate is not resolved in the FIM, but small clusters formed on this plane can be resolved, as can be seen in Figs. 13, 14, and 16. For clusters with five or fewer atoms, 1D and 2D structures can be observed with their relative probabilities dependent on the temperature, similar to clusters on the Ir(100). In contrast to the Ir(100), however, clusters with six or more atoms are formed right from the start at low temperatures as 2D clusters. Within the limited statistics of our observations, no linear chains of more than six atoms are observed. The image intensity of atoms in a cluster often varies considerably (as can be seen clearly in Figs. 13, 14, and 16), indicating that some of these atoms are protruded from the flat plane of the substrate. In other words, atoms in a cluster are not planar. The directions of some of the linear chains seem to deviate significantly from the $\langle 110\rangle$ directions of the atomic rows of the substrate. From the shape and the image intensity variations, a few structures of the clusters are proposed and are shown in Fig. 15. Geome-

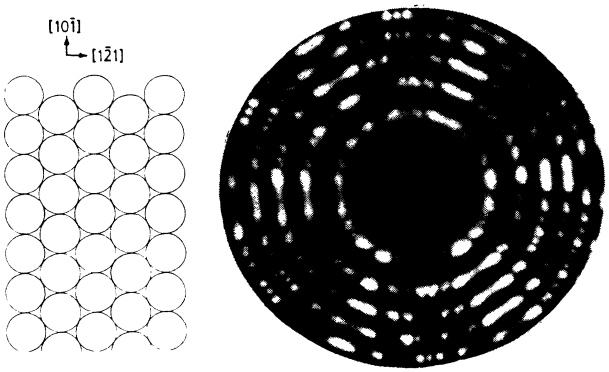

FIG. 12. The atomic and image structures of the Ir(111) surface.

trically highly symmetric cluster structures can be formed for clusters of seven and twelve atoms , as seen in Fig. 16. The formation of a large island from the coalescence of two large clusters is shown in Fig. 17. In this figure, one can also see Ir atoms in the terrace of the second layer gradually being absorbed into the edge of the top surface layer, and eventually forming a rather smoothed-out boundary after many periods of heating, or annealing.

All these atomic clusters can be gradually dissolved by dissociation of atoms if the surface temperature is high enough. The dissociation temperature, in general, increases nearly linearly with the size of the cluster, as already shown in Fig. 6. However, similar to the onset temperature of cluster diffusion, the three- and four-atom clusters are reversed in order also, signifying that the binding energy of the fourth atom to a three-atom cluster is smaller than that of the third atom to a two-atom cluster. This may arise from the nonmonotonic interadatomic interaction potential or the nonpairwise additivity of pair energies. It appears that this is a subject worthy of further investigation in the near future.

We have also carried out a careful measurement, out of a total of over 2000 heating periods of observations, of the temperature dependence of the 1D to 2D structure

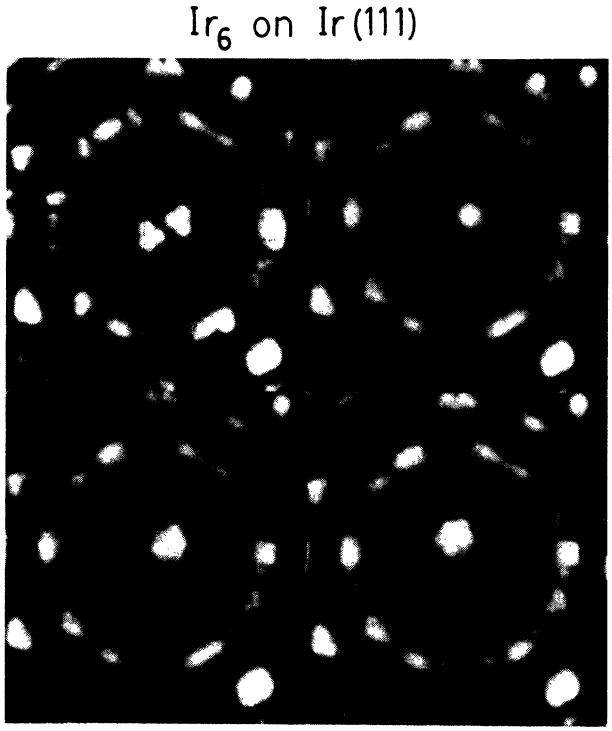

FIG. 14. Images showing formation of a six-atom Ir cluster and its structure changes on the Ir(111) surface.

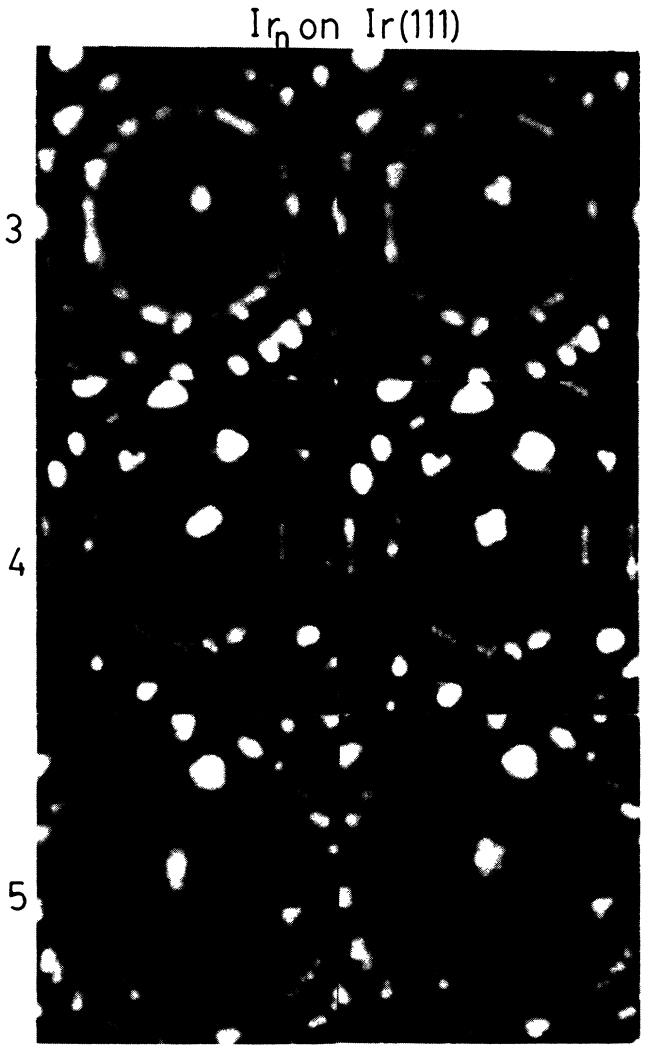

FIG. 13. Images of 1D and 2D cluster structures of three-, four-, and five-atom Ir clusters on the Ir(111) surface.

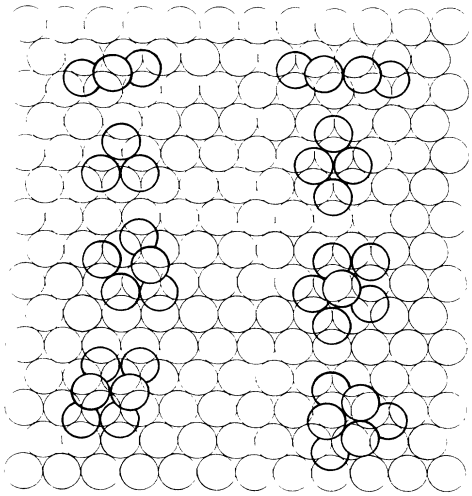

FIG. 15. Proposed structures of Ir clusters of three–six atoms.

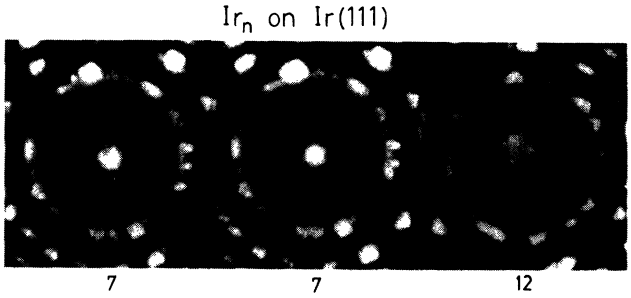

FIG. 16. Highly symmetric cluster structures can be formed for seven- and 12-atom Ir clusters on the Ir(111) surface.

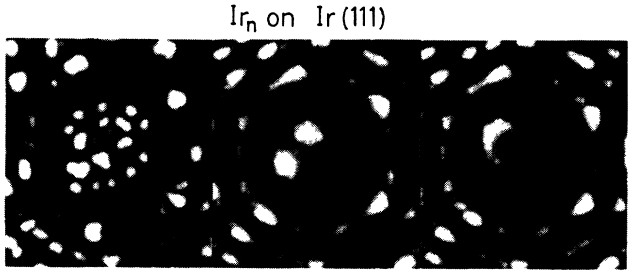

FIG. 17. Formation of two large Ir clusters and their coalescence into a large island on the Ir(111) surface.

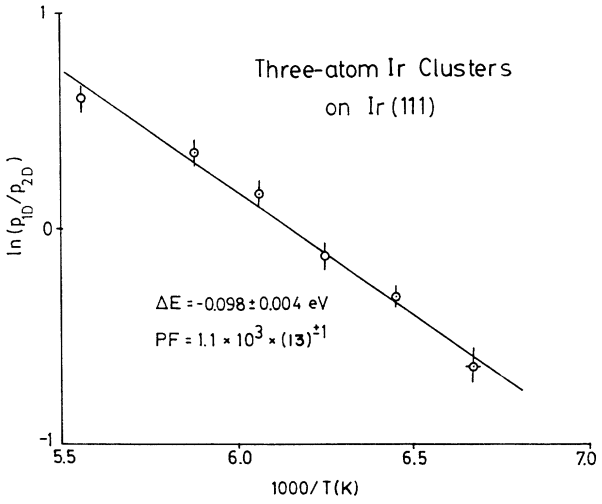

FIG. 18. The temperature dependence of the 1D to 2D structure transformation of three-atom Ir clusters on the Ir(111) surface.

transformation for the three-atom Ir cluster on the Ir(111) surface. In great contrast to the three-atom Ir cluster on the Ir(100) surface, the $\ln(p_{1D}/p_{2D})$ versus $1/T$ plot on the (111) surface shows a simple linear behavior, as can be seen in Fig. 18. From the slope and intercept of the plot, ΔE_{12} is derived to be -0.098 ± 0.004 eV, and the preexponential factor is found to be $1.1\times(10)^{\pm1.1}\times10^3$. The linearity of the plot is 0.9892. Thus on this plane, the 2D structure is more stable with a larger cluster binding energy of 0.098 ± 0.004 eV.

C. Dissociation of Ir(100) layers and 2D thermal desorption

When a field-ion emitter surface is heated to high temperatures, the size of a surface of lower surface free energy will increase from that of the field evaporation end form. This is achieved by a gradual thermal dissociation of atoms from the edges of the small top surface layers. This phenomenon is similar to the thermal desorption experiment of Taylor and Langmuir.[15] In their case, atoms, either lattice or adsorbed atoms, are thermally desorbed from the surface of a 3D crystal, whereas in the present case, lattice atoms are thermally desorbed from the edges of a surface layer. This may be called 2D thermal desorption or vaporization, or sublimation of a 2D crystal. It is possible to measure the dissociation energy of plane-edge atoms, or the 2D thermal desorption or sublimation energy by measuring the rate of decrease of the plane size as a function of the surface temperature. We have carried out a preliminary measurement for the Ir(100) surface.

When the Ir(100) surface is heated to high temperature, the 2D crystal shape, or the shape of the surface layer, changes from the more or less circular shape of the low-temperature field evaporation end form to a nearly square shape by diffusion of atoms along the layer edges. The sides of the square line up in the $\langle 110\rangle$ directions, or the closely packed atomic row directions. Following the idea of the 2D Wulff construction, the $\langle 110\rangle$ edges must have the lowest-line energy density of the 2D Ir(100) crystal. In addition, edge atoms are gradually dissociated from the top surface layer and the size of the layer gradually reduces, as shown in Fig. 19. These atoms will step down the lattice steps from the terraces and be absorbed into another surface layer elsewhere on the emitter surface. As the temperature where the dissociation rate becomes appreciable is very high, $\sim$500–700 K, and the terrace width is very narrow, one may assume that at the temperature of the measurements, diffusion of adatoms on the terrace is not a rate-limiting factor in the dissociation process. Therefore the rate of the loss of atoms from the top surface layer is given by

$$-\frac{dN}{dt}=\frac{2\pi r}{a}\nu_0\left[\frac{\exp(-E_d/kT)}{\exp(-E_d/kT)+\exp(-E_b/kT)}\right]\times\exp(-E_{\rm dis}/kT)\,, \tag{2}$$

where r is the radius of the top surface layer, a is the diameter of the atoms, E_b is the barrier height at the boundary of the terrace of the second surface layer (the

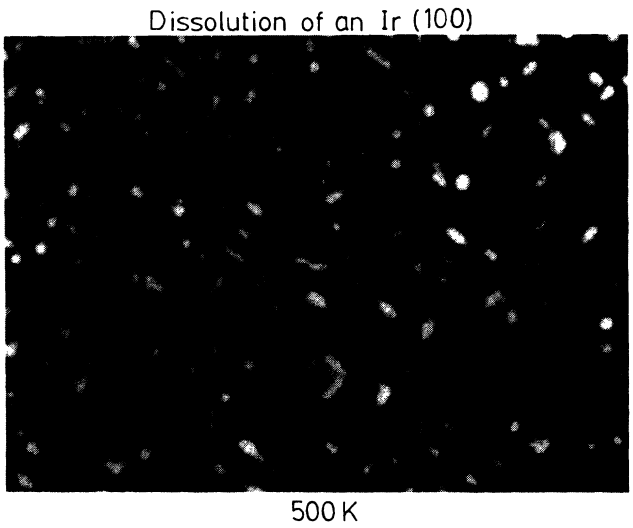

FIG. 19. A gradual thermal dissociation of a top (100) layer of an Ir tip at 500 K.

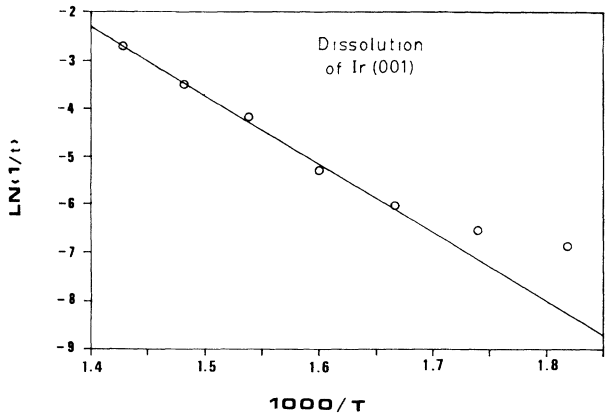

FIG. 20. $\ln(1/\tau)$-vs-$(1/T)$ plot in the thermal dissociation of the top (100) layer of an Ir tip.

boundary is, in general, reflective), $E_{\rm dis}$ is the dissociation energy of plane-edge atoms, E_d is the activation energy of surface diffusion of single atoms on the terrace, N is the number of atoms remaining in the top surface layer, and ν_0 is the preexponential factor of the dissociation process. By integrating this equation from 0 to τ and from R_0 to 0, where R_0 is the initial radius of the circularly shaped top surface layer, one obtains

$$\frac{1}{\tau}=\frac{\nu_0}{R_0}\frac{\exp[-(E_{\rm dis}+\Delta E_b)/kT]}{[1+\exp(-\Delta E_b/kT)]}\ , \tag{3}$$

where $\Delta E_b=E_b-E_d$ is the extra barrier height of the reflective boundary. From earlier measurements it is estimated that ΔE_b is of the order of 0.1–0.2 eV, or $\Delta E_b \gg kT$.[4,16] Equation (3) can be rearranged to

$$\ln\left[\frac{1}{\tau}\right]=\ln\left[\frac{\nu_0}{R_0}\right]-\frac{E_{\rm dis}+\Delta E_b}{kT}\ . \tag{4}$$

Thus, within the validity of the approximation, by plotting the logarithm of the inverse time of dissociation against the inverse temperature, a linear plot can be expected, with its slope representing the sum of the dissociation energy and the extra barrier height of the boundary. A set of data is shown in Fig. 20. At high temperatures, the plot is indeed linear, but at low temperatures, it deviates significantly. The slope gives $E_{\rm dis}+\Delta E_b \sim 1.4$ eV. For Ir on Ir(100), the boundary is nonreflective, or $\Delta E_b=0$. Thus the dissociation energy of plane-edge atoms from the Ir(100) layer is ~ 1.4 eV. The significant deviation from the linear behavior observed at low temperatures indicates that surface diffusion at the terrace may affect significantly the dissociation rate of the surface layer at low temperatures.

The binding energy of kink-site atoms is identical to the cohesive energy of the solid. This can be easily understood. Kink sites are where one can remove all the atoms in a solid with an identical atomic environment, i.e., exactly one half the coordination numbers of a bulk atom, thus one needs the same energy to remove every atom in the solid. This energy, by definition, is the cohesive energy of the solid. The binding energy of an adatom on a surface should be equal to the cohesive energy minus the dissociation energy of the kink site atom, then plus the activation energy of surface diffusion of adatoms on that plane.[12,17] Thus it is possible to determine the binding energy of an adsorbed atom on a surface plane by simply measuring the dissociation energy of kink site atoms as both the cohesive energy and the activation energy of surface diffusion are already known.

There are three different sites, i.e., kink sites, ledge sites and edge sites, as shown in Fig. 21, from which plane-edge atoms can be dissociated from the surface layer. In 2D thermal desorption of a surface layer, unless the temperature is very high, atoms are dissociated from the plane edges in an orderly manner, as can be seen from Fig. 19. This is possible only if edge atoms are removed first, followed by kink atoms, and finally ledge atoms, etc. As the numbers of edge and ledge atoms are much less

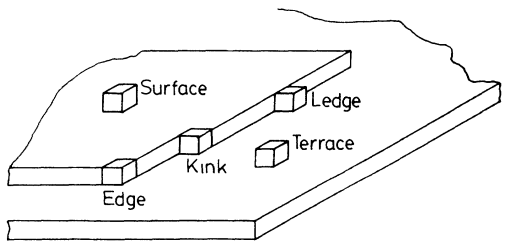

FIG. 21. At the edges of a surface layer, there exist three different types of atomic sites. They are the edge site, ledge site, and kink site. A kink-site atom has exactly half the coordination numbers of a bulk atom.

than that of kink atoms, the 2D thermal desorption rate is mainly determined by the thermal desorption rate of kink atoms. Thus the 2D thermal desorption energy $E_{\rm dis}$ derived should well approximate the dissociation energy of kink-site atoms. With this argument, the dissociation energy of kink-site atoms of the Ir(100) surface should be ~ 1.4 eV. The binding energy of an Ir adatom on the Ir(100) surface is then given by $E_c + E_d - E_{\rm dis} = (6.94 + 0.93 - 1.4)$ eV $\simeq 6.5$ eV. As far as we are aware, this is the first time a reasonably reliable binding energy of a metal adatom on a surface, an Ir on the Ir(100) surface, has been obtained. With regard to finding the exact sites from which atoms are dissociated from the surface layer edge, it may be possible to use a ns pulsed-laser heating technique, similar to an FIM study of the atomic steps involved in the surface atomic reconstruction.[18]

IV. SUMMARY

Several atomic processes on Ir surfaces have been studied using the field-ion microscope, and quantitatively reliable data have been obtained for surface diffusion, structure transformation of three-atom Ir clusters on the Ir(111) and Ir(100) surfaces, and the 2D thermal desorption of the top (100) surface layer. From these data, the energetics of these atomic processes have been investigated. For some other processes, data presented are either semiquantitative or qualitative, thus further studies are needed. In general, the binding energy of surface atoms with the substrate is of the order of a few eV, the same order of magnitude as the cohesive energy of the solid. The diffusion barrier of single atoms on the surface is an order of magnitude smaller, or a few tenths of an eV. The interaction between adatoms and between an adatom and a small cluster is on the order of a few tens meV, or another order of magnitude smaller.

An interesting feature we have found is that the 1D to 2D structure transformation of the three-atom Ir cluster is very different on the Ir(111) surface and on the Ir(100) surface. On the Ir(111) surface, the $\ln(p_{\rm 1D}/p_{\rm 2D})$ versus $1/T$ plot exhibits a simple linear behavior, while on the Ir(100) plot, this plot deviates significantly from the linearity at low temperatures. While all our experimental measurements are done below 420 K, where no surface reconstruction occurs, the energetics involved in this peculiar structure transformation behavior of the three-atom cluster on the Ir(100) surface may be intimately related to the energetics of the atomic reconstruction of this surface. It is well known that the Ir(100) surface transforms into a quasihexagonal (1×5) structure above 900 K.[19] Further investigation of the energetics of structure transformation of larger Ir clusters on this surface should be able to clarify the energetics of this surface reconstruction.

ACKNOWLEDGMENTS

This work was supported by the National Science Foundation (NSF). The authors acknowledge Tom Eskew for developing the pulsed dc power supply used for tip heating in this experiment.

[1]A. Zangwill, *Physics at Surfaces* (Cambridge Univ. Press, Cambridge, (1988); E. Bauer, in *The Chemical Physics of Solid Surfaces and Heterogeneous Catalysis*, edited by D. A. King and D. P. Woodruff (Elsevier, New York, 1984), Vol. 3.

[2]J. P. Hirth and G. M. Pound, *Condensation and Evaporation, Nucleation and Growth Kinetics, in Prog. Mater. Sci. Vol. II* (Pergamon, New York, 1963).

[3]See, for example, E. W. Müller and T. T. Tsong, *Field Ion Microscopy, Principles and Applications* (Elsevier, New York, 1969).

[4]See, for examples, G. Ehrlich and K. Stolt, Annu. Rev. Phys. Chem. **31**, 603 (1980); D. W. Bassett, in *Surface Mobilities on Solid Materials*, edited by T. Binh (Plenum, New York, 1981); T. T. Tsong, Rep. Prog. Phys. **51**, 759 (1988); Surf. Sci. Rep. **8**, 127 (1988).

[5]G. Ayrault and G. Ehrlich, J. Chem. Phys. **60**, 281 (1974).

[6]R. T. Tung and W. R. Graham, Surf. Sci. **97**, 73 (1980).

[7]P. R. Schwoebel and G. L. Kellogg, Phys. Rev. Lett. **61**, 578 (1988).

[8]See, for example, J. D. Doll and A. F. Voter, Annu. Rev. Phys. Chem. **38**, 413 (1987).

[9]H. F. Liu, H. M. Liu, and T. T. Tsong, J. Appl. Phys. **59**, 1334 (1986).

[10]G. L. Kellogg and T. T. Tsong, J. Appl. Phys. **51**, 1184 (1980).

[11]T. F. Page and B. Ralph, Nature (London), Phys. Sci. **234**, 163 (1971).

[12]G. L. Kellogg, T. T. Tsong, and P. L. Cowan, Surf. Sci. **70**, 485 (1978).

[13]See Figs. 7(g)–7(i) of T. T. Tsong, Phys. Rev. B **6**, 417 (1972).

[14]D. W. Bassett, Thin Solid Films **48**, 237 (1978).

[15]J. B. Taylor and I. Langmuir, Phys. Rev. **44**, 423 (1933).

[16]S. C. Wang and T. T. Tsong, Surf. Sci. **121**, 85 (1982).

[17]T. T. Tsong, Y. Liou, and J. Liu, J. Vac. Sci. Technol. A **7**, 1758 (1989).

[18]Q. J. Gao and T. T. Tsong, Phys. Rev. Lett. **57**, 452 (1986).

[19]E. Lang, K. Müller, H. Heinz, M. A. van Hove, R. J. Koestner, and G. A. Somorjai, Surf. Sci. **127**, 347 (1983).

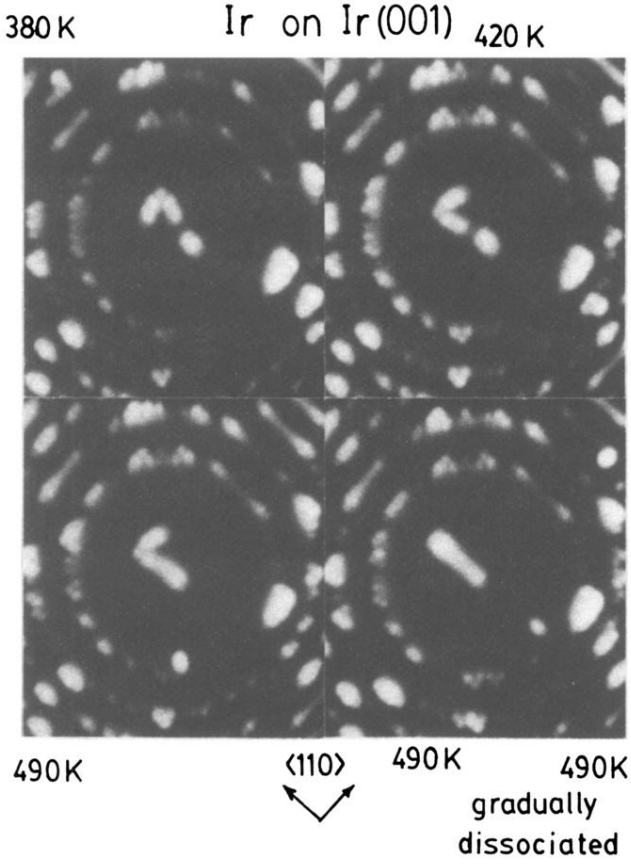

FIG. 10. Image of a nine-atom Ir cluster on the Ir(100) surface showing various stages of structure changes.

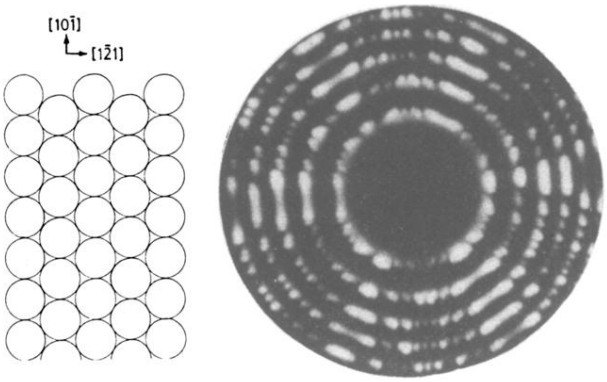

FIG. 12. The atomic and image structures of the Ir(111) surface.

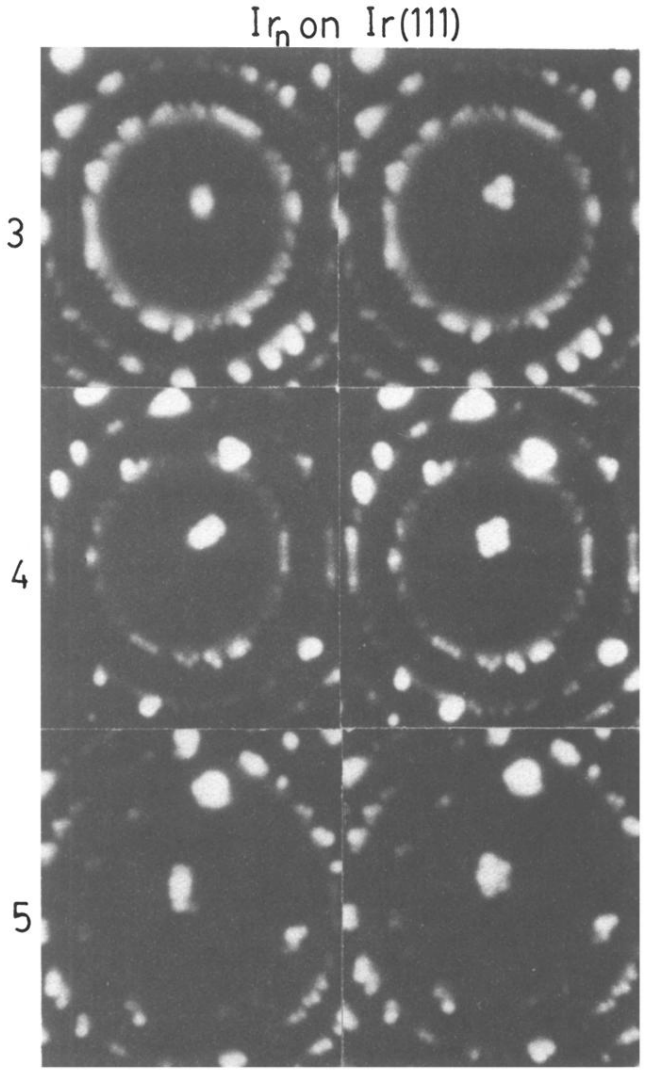

FIG. 13. Images of 1D and 2D cluster structures of three-, four-, and five-atom Ir clusters on the Ir(111) surface.

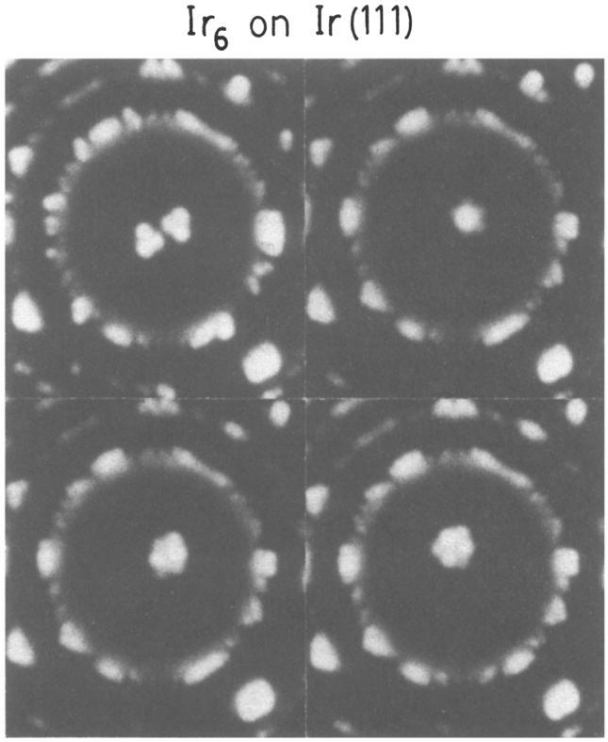

FIG. 14. Images showing formation of a six-atom Ir cluster and its structure changes on the Ir(111) surface.

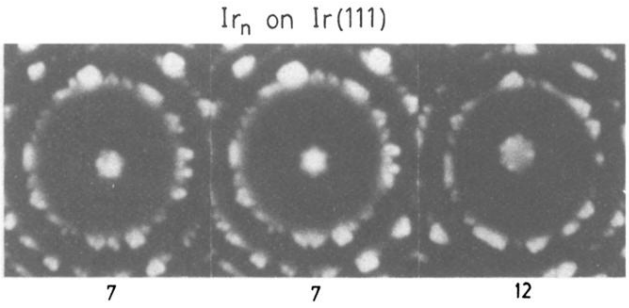

FIG. 16. Highly symmetric cluster structures can be formed for seven- and 12-atom Ir clusters on the Ir(111) surface.

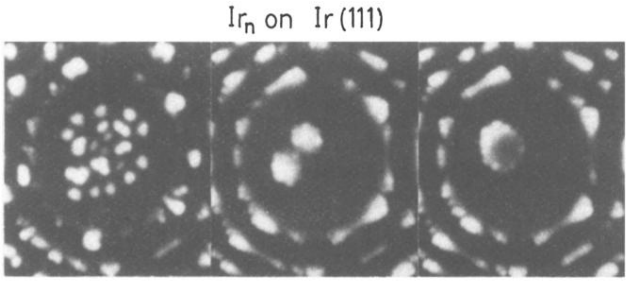

FIG. 17. Formation of two large Ir clusters and their coalescence into a large island on the Ir(111) surface.

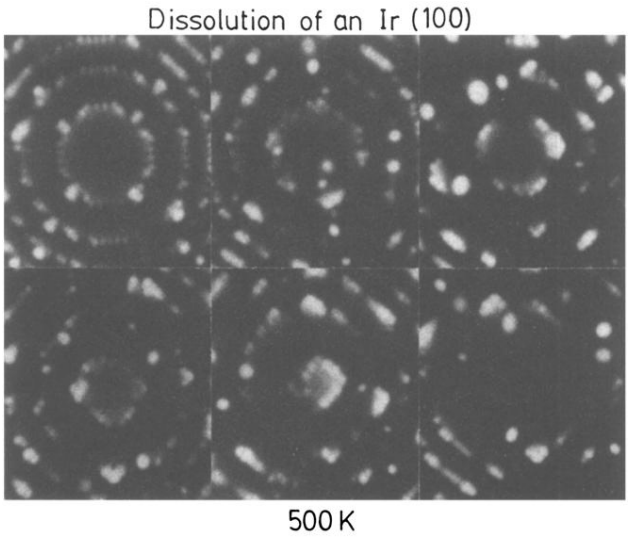

FIG. 19. A gradual thermal dissociation of a top (100) layer of an Ir tip at 500 K.

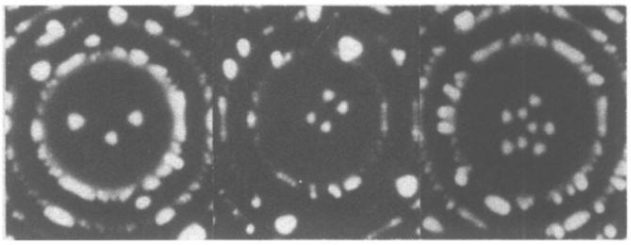

FIG. 3. A few helium-ion micrographs showing the triangular image spots for Ir adatoms on the Ir(111) surface.

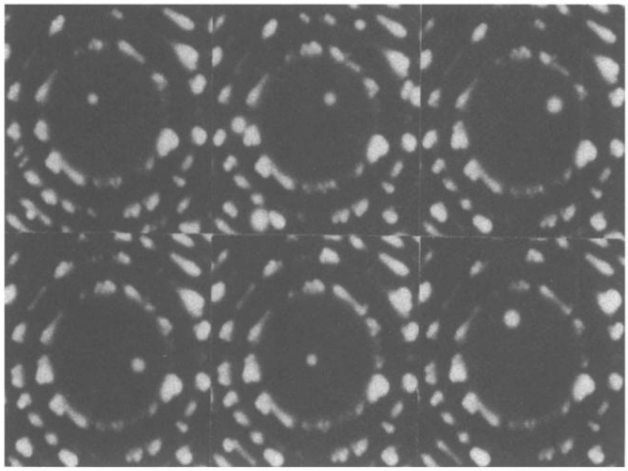

FIG. 4. FIM images showing 2D random walk surface diffusion of an Ir adatom on an Ir(100) surface.

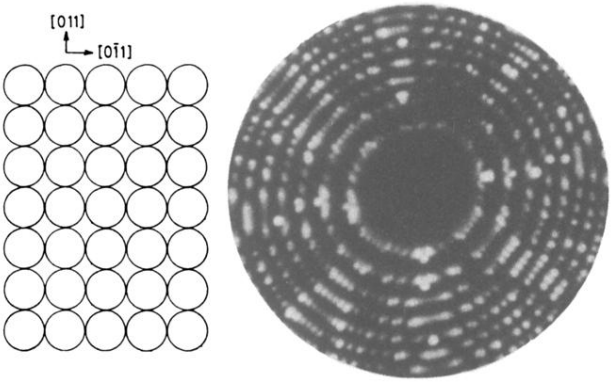

FIG. 7. The atomic and image structures of the Ir(100) surface. Each ring represents a surface layer.

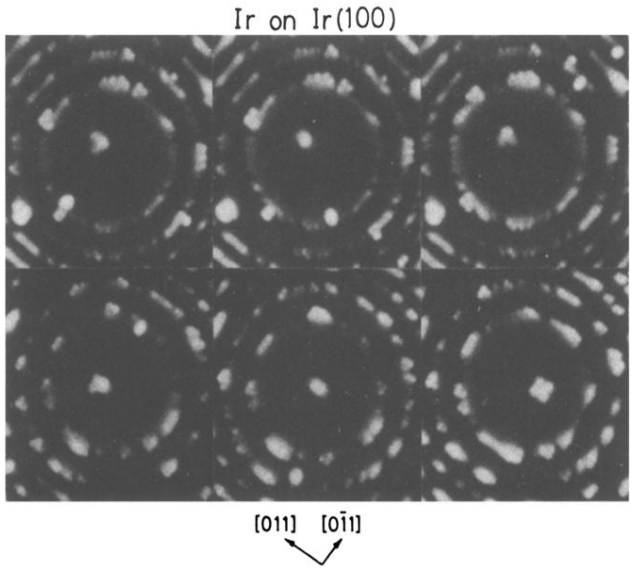

FIG. 8. Images of three- and four-atom Ir clusters on the Ir(100) surface. In a field-ion image, the magnification of a small atomic cluster is usually much larger than the overall magnification of the image.

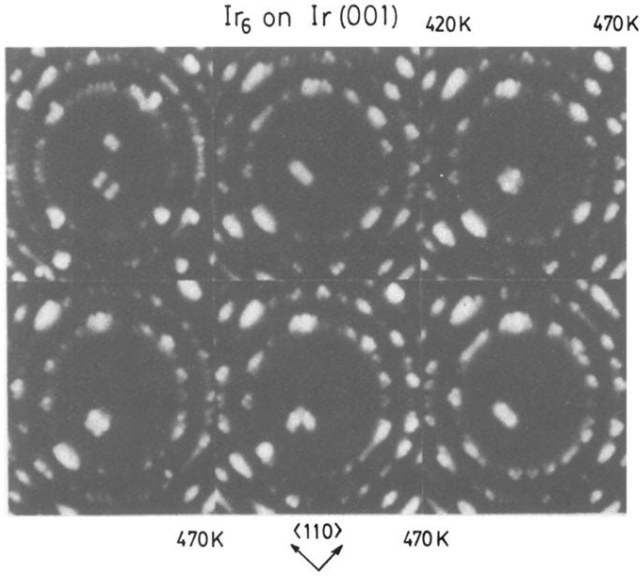

FIG. 9. Images of a six-atom Ir cluster on the Ir(100) surface and its structure changes at different heating temperatures.